

Deflagration-to-Detonation Transition in Laser-Ignited Explosive Gas Contained in a Smooth-Wall Tube

T. Endo, K. Okada, S. Kuwajima, W. Kim, T. Johzaki, D. Shimokuri, A. Miyoshi, and S. Namba
Department of Mechanical Systems Engineering, Hiroshima University
Higashi-Hiroshima, Hiroshima, Japan

1 Introduction

Detonation is an important combustion mode from the viewpoint of not only safety but also applications because of its high pressure and temperature. In most cases, detonation is formed from deflagration through the process so-called deflagration-to-detonation transition (DDT). The typical scenario of DDT is as follows [1].

- (1) Ignition and initial flame-kernel development into quasi-planar flames.
- (2) Flame acceleration due to the wrinkling of the unstable flame front.
- (3) Choked-flame propagation at the Chapman-Jouguet deflagration speed.
- (4) Detonation onset triggered by micro-explosions in a shock-flame complex.

An ignition method can influence significantly the first step mentioned above, and such an ignition method that promotes the initial flame-kernel development and subsequent DDT process is suitable for detonation applications.

In fact, compared with ordinary spark-plug ignition, laser ignition can deposit larger energy in a smaller region of combustible gas in shorter duration, and therefore can result in a larger initial flame kernel and its earlier development [2]. In this research, for clarifying whether this characteristic of laser ignition leads the promotion of DDT or not, we investigate the influence of the position and energy of laser ignition on DDT in a smooth-wall tube.

2 Experimental arrangement

The experimental arrangement is shown in Fig. 1. The combustor, the inner diameter and thickness of which are 20 mm and 10 mm, respectively, consists of a 940-mm-long tube made of polymethyl methacrylate (PMMA) and a 60-mm-long tube made of brass. One end of the combustor is closed and the other end is connected to a large tank, the inner diameter and length of which are 208.3 mm and 520 mm,

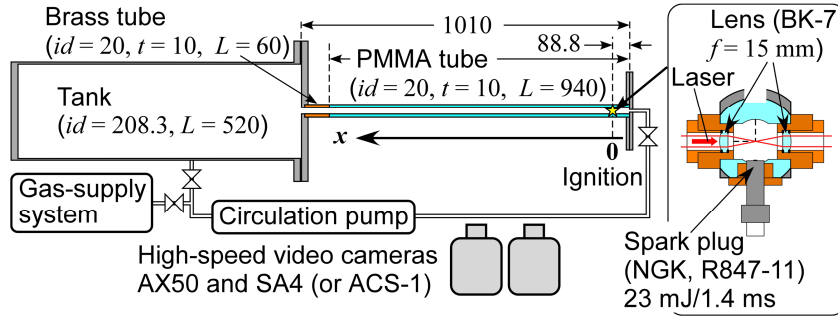


Fig. 1 Experimental arrangement.

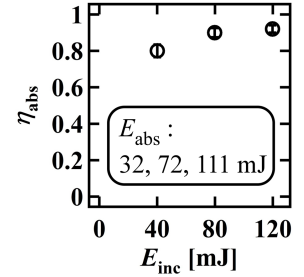


Fig. 2 Laser absorption.

respectively. A gas-feeding pipe, the inner diameter of which is 3.6 mm, is connected to the closed end of the combustor. The PMMA tube is contained in a larger stainless-steel pipe, which has observation windows, for safety's sake. The explosive gas used in the present experiments was $0.87[(1/4)\text{C}_2\text{H}_4 + (3/4)\text{O}_2] + 0.13\text{N}_2$, which was initially quiescent at 100 kPa and about 20 °C, and premixed using a circulation pump.

Figure 1 also shows the ignition arrangement. The gas was ignited at 88.8 mm from the closed end of the PMMA tube. In the case of laser ignition, the gas was ignited near the center axis of the tube. When we used a semi-surface-discharge-type spark plug (NGK, R847-11) and an automobile spark-plug driver (TOYOTA, 90919-02240) for ignition, the gas was ignited near the inner surface of the tube. In the case of the spark-plug ignition, we measured the discharge voltage $V(t)$ using a high-voltage probe (Tektronix, P6015A) and the discharge current $I(t)$ using a current probe (Magnetlab, CT-B0.5), and evaluated the discharge energy E_{sp} by the formula $E_{sp} = \int_{t_1}^{t_2} (V - r_i I) Idt$, where $r_i (= 5963 \Omega)$ was the internal resistance of the spark plug, t_1 was the time at which the discharge current began to flow, and t_2 was the time at which the discharge current ended to flow. As a result of the evaluation, E_{sp} was approximately 23 mJ, and the discharge duration ($t_2 - t_1$) was approximately 1.4 ms. Regarding the laser pulse, its wavelength was 1064 nm (Nd:YAG), its duration was approximately 12 ns, which was shorter than the discharge duration of the spark plug five orders in magnitude, its beam diameter before focusing was approximately 5 mm, and it was focused by a 15-mm-focal-length plano-convex lens made of BK7 optical glass on the center axis of the tube. In the case of the laser ignition, we measured the incident laser energy (E_{inc}) and the transmitted laser energy (E_{tra}), and thereby calculated the absorbed laser energy ($E_{abs} = E_{inc} - E_{tra}$). In the experiments, the incident laser energy was varied as 40, 80, 120 mJ. The laser absorption efficiencies ($\eta_{abs} = E_{abs}/E_{inc}$) and the absorbed laser energies are summarized in Fig. 2.

In order to investigate DDT process, we observed the visible self-emission from the reacting and/or hot gas in the PMMA tube side-on using high-speed video cameras (Photron, AX50; Photron, SA4; and nac, ACS-1). Using AX50 and appropriate neutral-density (ND) filters, we observed deflagration at the frame rate of 2×10^4 fps and with the exposure time of 10 μs . Using SA4 and appropriate ND filters, we observed detonation at the frame rate of 2×10^4 fps and with the exposure time of 1 μs . ACS-1 is a high-performance high-speed video camera with wide dynamic range, and was temporarily used by courtesy of nac Image Technology Inc. for observing the whole DDT process by a single camera at the frame rate of 2×10^5 fps and with the exposure time of 1 μs . In order to determine the flame-front position in each image, we first depicted the exposure profile along the center axis of the PMMA tube, and subsequently

defined the position of the flame front as the position at which the slope of the exposure profile was the maximum.

In the present experiments, as shown in Fig. 3(a), a nylon spacer, which had a hole of 5-mm in inner diameter along its axis, was installed at the closed end of the PMMA tube in some cases. Thereby the effective distance between the ignition position and the tube end was varied as 8 and 88.8 mm as shown in Fig. 3.

3 Results and discussion

3.1 The case of ignition at 8 mm from the tube end

The flame speed in the laboratory frame obtained from the temporal evolution of the experimentally determined flame-front position is shown in Fig. 4 as a function of time. In Fig. 4, the Chapman-Jouguet detonation speed ($D_{CJ} = 2297.8$ m/s [3]) is shown by the horizontal solid line labelled ‘‘Steady detonation,’’ the sound speed of the isobarically burned gas ($a_b = 1094.4$ m/s [3]) is shown by the horizontal dash-dot line labelled ‘‘Choked flame,’’ and the speed of the planar laminar flame in the laboratory frame ($S_{u,L} \rho_u / \rho_b = 50.696$ m/s) is shown by the horizontal broken line labelled ‘‘Planar laminar flame,’’ where $S_{u,L} (= 3.7251$ m/s) and $\rho_u / \rho_b (= 13.609)$ [4,5] are the burning velocity and volume expansion ratio of the planar laminar flame, respectively.

Although the larger laser energy resulted in the earlier detonation onset, it seems that the scenario of DDT was almost the same as the typical one described previously. As shown in Fig. 4, the larger laser energy resulted in the earlier flame acceleration. This seems the reason why the larger laser energy results in the earlier detonation onset.

We defined the run-up time to DDT (t_{DDT}) as the time at which the flame acceleration in the laboratory frame is the maximum, and the run-up distance to DDT (x_{DDT}) as the position of the flame front at t_{DDT} . The experimentally-obtained values of t_{DDT} and x_{DDT} are summarized in Table 1, where the percentage of each value compared with the case that the gas was ignited by the spark plug is shown in the parenthesis. Although DDT was promoted by laser ignition with large energy, it was not significant. This is because the scenario of DDT was essentially the same as in the case of the spark-plug ignition.

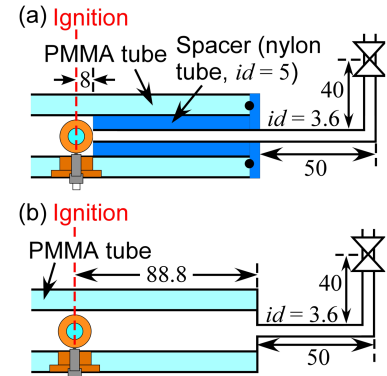


Fig. 3 Ignition positions.

(a) 8 mm from the tube end.

(b) 88.8 mm from the tube end.

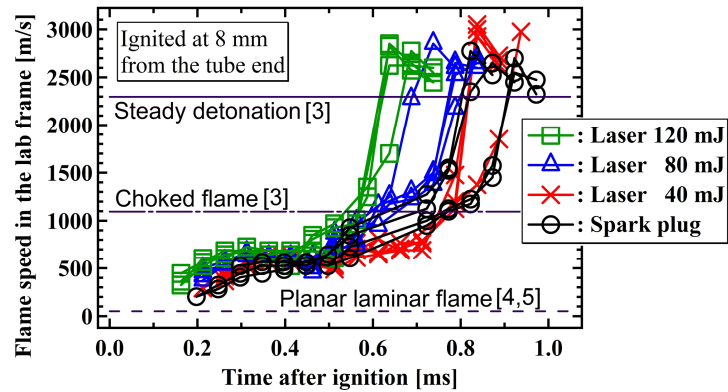


Fig. 4 Temporal evolution of the flame speed in the case of ignition at 8 mm from the tube end.

Table 1 Run-up time and distance to DDT in the case of ignition at 8 mm from the tube end

Ignition	t_{DDT} [ms]	x_{DDT} [mm]
Spark plug	0.85 ± 0.06 (100%)	482 ± 41 (100%)
Laser 40 mJ	0.84 ± 0.05 (99%)	471 ± 60 (98%)
Laser 80 mJ	0.74 ± 0.05 (87%)	453 ± 68 (94%)
Laser 120 mJ	0.63 ± 0.03 (74%)	427 ± 51 (89%)

3.2 The case of ignition at 88.8 mm from the tube end

The flame speed in the laboratory frame is shown in Fig. 5 as a function of time. In the case of ignition at 88.8 mm from the tube end, two scenarios of DDT were observed. The first scenario is the typical one previously described. In contrast, in the second scenario, the detonation onset occurred before the flame was accelerated to the choked flame. As shown in Fig. 5, the second scenario was observed in all experiments where the incident laser energy was 120 mJ, but never observed in all experiments where the gas was ignited by the spark plug. In addition, it seems that the second scenario was more frequently observed and the detonation onset occurred earlier for the larger laser energy.

The experimentally-obtained values of t_{DDT} and x_{DDT} in the case of ignition at 88.8 mm from the tube end are summarized in Table 2, where the percentage of each value compared with the case that the gas was ignited by the spark plug at 8 mm from the tube end (shown in Table 1) is shown in the parenthesis. As shown in Table 2, in the case of the second scenario, both the run-up time and distance to DDT (t_{DDT} and x_{DDT}) are shortened significantly. Furthermore, the promotion of DDT was more significant for the larger laser energy.

Figure 6 shows the sequential self-emission images obtained by the high-speed video camera (ACS-1) in the case of 120-mJ laser ignition at 88.8 mm from the tube end. In this case, the detonation onset occurred at about 0.420 ms. As shown in Fig. 6, we can recognize a shock wave propagating in the burned gas and following the flame front in the images at the times before 0.420 ms. And the detonation onset occurred almost the same time as the shock wave caught up with the flame front. The temporal evolution of the positions of the flame fronts and the shock wave obtained from the images shown in Fig. 6 is shown in Fig. 7, where the temporal evolution of the position of the flame front propagating toward the closed tube end (namely toward the negative x direction) is also plotted. As shown in Fig. 7, the shock wave began to be observed a little after the time at which the flame front propagating toward the closed tube end was hidden by the flange at the tube end. Therefore, the shock wave is considered to be generated by the end-gas autoignition similarly to engine knock [6,7] near the tube end or inside the gas-feeding pipe connected to the tube end. In Fig. 7, M_{IS} denotes the

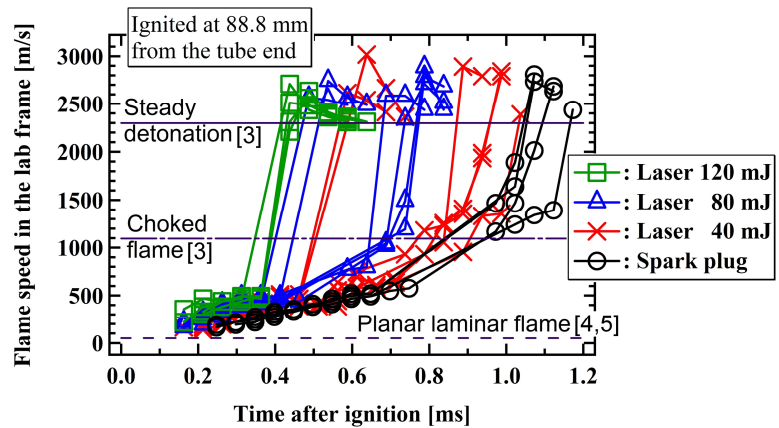


Fig. 5 Temporal evolution of the flame speed in the case of ignition at 88.8 mm from the tube end.

Table 2 Run-up time and distance to DDT in the case of ignition at 88.8 mm from the tube end

Ignition	In the case of the first scenario		In the case of the second scenario	
	t_{DDT} [ms]	x_{DDT} [mm]	t_{DDT} [ms]	x_{DDT} [mm]
Spark plug	1.09 ± 0.05 (128%)	534 ± 50 (111%)	<i>Not observed</i>	
Laser 40 mJ	0.95 ± 0.05 (112%)	491 ± 93 (102%)	0.59 ± 0.03 (69%)	292 ± 17 (61%)
Laser 80 mJ	0.73 ± 0.05 (86%)	342 ± 57 (71%)	0.49 ± 0.04 (58%)	284 ± 16 (59%)
Laser 120 mJ	<i>Not observed</i>		0.43 ± 0.03 (51%)	187 ± 53 (39%)

propagation Mach number of the incident shock wave on the flame front, assuming a shock wave propagating in the isobarically burned gas at rest. In fact, we recognized one or two shock waves following the flame front in every experiment, in which we used the wide-dynamic-range high-speed video camera (ACS-1), including the cases of ignition at 8 mm from the tube end. However, only in the case of $M_{IS} \geq 1.8$, the detonation onset occurred almost the same time as the shock wave caught up with the flame front, and the second scenario of DDT was observed. From this fact, we interpret the second scenario of DDT as follows. In the case that the gas is ignited by laser with relatively large energy at slightly away from the closed tube end, the flame propagating toward the closed tube end is strongly accelerated, and consequently a shock wave generated by the end-gas autoignition becomes strong. If the condition $M_{IS} \geq 1.8$ is satisfied, where this condition probably depends on the experimental conditions, the shock wave following the flame front is strong enough to induce the detonation onset by catching up with the flame front even if the flame speed is still slower than the choked flame.

For the case that a shock wave collides with the flame front from the burned-gas side toward the unburned-gas side, the strength of the transmitted shock wave in the unburned gas is evaluated treating the flame front as an ordinary contact discontinuity through which no gas passes [8]. The evaluation results are shown in Fig. 8, where M_{TS} , T_{TS} , and Δu_{TS} denote the propagation Mach number, induced temperature, and induced flow speed regarding the transmitted shock wave in the unburned gas, respectively. The incident shock wave of $M_{IS} = 1.8$ corresponds to the transmitted shock wave of $M_{TS} = 2.4$, $T_{TS} = 570$ K, and $\Delta u_{TS} = 560$ m/s. The shock-induced unburned-gas temperature of 570 K seems to be too low to initiate micro-explosions inducing the detonation onset. Therefore, the mixing of the unburned and burned gases induced by Richtmyer-Meshkov instability at the flame front is the most plausible mechanism for initiating micro-explosions inducing the detonation onset.

4 Conclusions

DDT process subsequent to laser ignition was experimentally studied varying the incident laser energy, where the explosive gas was ignited at 8 or 88.8 mm from the closed tube end. The DDT process in the case of ignition near the closed tube end was as follows. Although laser ignition promoted DDT, it was not significant. This is because the scenario of DDT was essentially the same as the typical one. The DDT process in the case of ignition slightly away from the closed tube end was as follows. Two scenarios of DDT were observed. The first scenario was the typical one. In the second scenario, the detonation onset

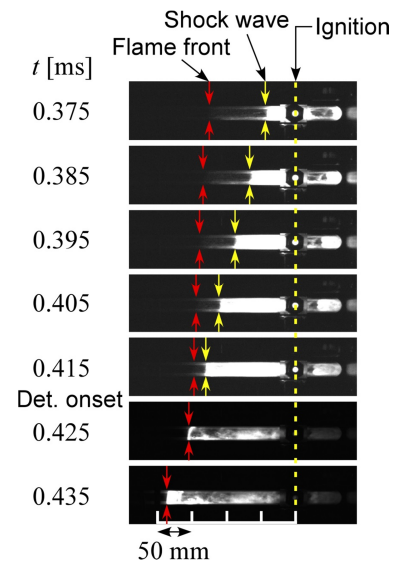


Fig. 6 Self-emission images observed by ACS-1 (high-speed video camera) in the case that the gas was ignited at 88.8 mm from the tube end by 120-mJ laser.

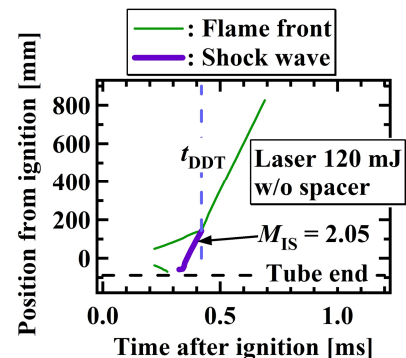


Fig. 7 Trajectories of flame fronts and shock wave in the case that the gas was ignited at 88.8 mm from the tube end by 120-mJ laser.

was induced in the abnormally early phase by a shock wave following the flame front. Significant DDT promotion was realized in the second scenario by laser ignition. The shock wave was probably generated by the end-gas

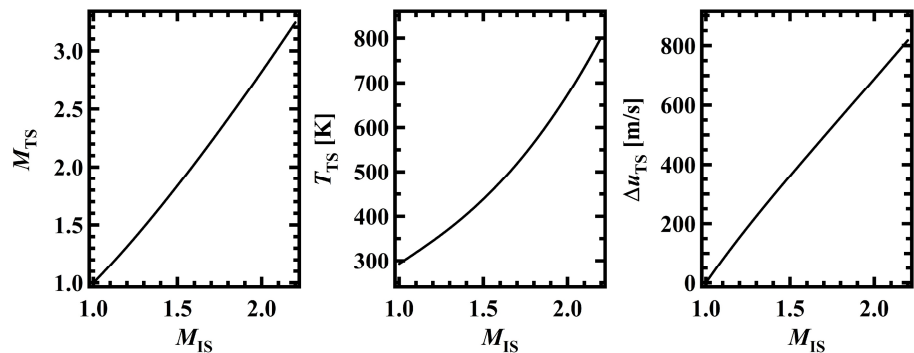


Fig. 8 Evaluation results on the transmitted shock wave.

autoignition, and was more strongly driven by the larger laser energy through the more promoted flame acceleration. The mixing of the unburned and burned gases induced by Richtmyer-Meshkov instability at the flame front is the most plausible mechanism for initiating micro-explosions inducing the detonation onset.

Acknowledgments

This work was supported by JSPS KAKENHI Grant Number JP17H03482. A high-performance high-speed video camera (ACS-1) was used by courtesy of nac Image Technology Inc.

References

- [1] Ciccarelli G, Dorofeev S. (2008). Flame acceleration and transition to detonation in ducts. *Prog. Energy Combust. Sci.* 34: 499.
- [2] Endo T, Takenaka Y, Sako Y, Johzaki T, Namba S, Shimokuri D. (2017). An experimental study on the ignition ability of a laser-induced gaseous breakdown. *Combust. Flame.* 178: 1.
- [3] Gordon S, McBride BJ. (1996). Computer Program for Calculation of Complex Chemical Equilibrium Compositions and Applications. NASA Reference Publication 1311.
- [4] <http://www.ansys.com/products/fluids/ansys-chemkin-pro>.
- [5] Metcalfe WK, Burke SM, Ahmed SS, Curran HJ. (2013). A Hierarchical and Comparative Kinetic Modeling Study of C_1 – C_2 Hydrocarbon and Oxygenated Fuels. *Int. J. Chem. Kinet.* 45: 638.
- [6] Yu H, Chen Z. (2015). End-gas autoignition and detonation development in a closed chamber. *Combust. Flame.* 162: 4102.
- [7] Qi Y, He X, Wang Z, Wang J, Zhang H, Jiang Y. (2015). An experimental investigation of super knock combustion mode using a one-dimensional constant volume bomb. *Int. J. Hydrogen Energy.* 40: 2377.
- [8] Igra O. (2001). One-Dimensional Interactions. In *Handbook of Shock Waves*, Vol. 2, Ch. 7, Academic Press, San Diego (ISBN 978-0120864300).